# Surface energy and adhesion energy of solution-based patterning in organic thin film transistors

Hsiao Wen Zan [a,*], Cheng-Wei Chou [b], Kuo-Hsi Yen [b]

[a] *Department of Photonics & Display Institute, National Chiao Tung University, 1001 Ta-Hsueh Rd., 300 HsinChu, Taiwan, Republic of China*
[b] *Department of Photonics & Institute of Electro-Optical Engineering, National Chiao Tung University, HsinChu, Taiwan, Republic of China*

## Abstract

This study elucidates the patterning of pentacene by adjusting its surface energy. The surface energy was modified by self-assembled monolayer treatment and exposure to ultra-violet (UV) light through a quartz-glass mask. Then, following pentacene deposition, dipping in water was used to remove pentacene from the UV-exposed area. The adhesion energy and the intrusion energy were analyzed to determine the mechanism of this patterning process. The variation of the intrusion energy with the surface energy was found to be the main issue in pentacene patterning. The characteristics of pentacene-organic thin film transistors were also measured to confirm the proposed method.
© 2007 Elsevier B.V. All rights reserved.

*Keywords:* Pentacene; Surface energy; SAM

## 1. Introduction

The pentacene-based organic thin film transistor (OTFT) has received much attention because it is fabricated at low temperatures on plastic substrates at low cost [1–3]. Carrier transport in pentacene-based OTFT is generally dominated by the characteristics of the interface between the pentacene film and the gate dielectric [4,5]. Numerous studies of the self-assembly monolayer (SAM) have been performed to modify effectively the gate dielectric surface to improve carrier mobility [6,7]. The SAM layer changed the gate dielectric surface from hydrophilic to hydrophobic, enabling the pentacene molecules to align vertically to form the π-orbital. Additionally, given suitable process design, the difference between the hydrophilic and hydrophobic properties is important in the patterning of an organic film [7–9].

Recently, Masahiko Ando et al. demonstrated a simple method for controlling surface polarity (hydrophilic or hydrophobic) using an SAM layer and exposure to ultra-violet (UV) light to pattern the pentacene film [10]. However, the details of the variation of the surface energy have not been discussed. The method left the unwanted high-resistivity pentacene film around the pentacene channel; this may cause cross-talk and the flow of leakage current in OTFT array. Furthermore, the exposure of the backside to UV light depends on a highly transmitting substrate, such as quartz-glass. Such a substrate limits the range of applications since several plastic substrates do not exhibit high transmissivity. This study develops a top-exposure method that can be easily combined with conventional lithography using a quartz mask. The film was dipped into de-ionized (D.I.) water to remove the unwanted pentacene film and prevent crosstalk and the flow of leakage current. The interfacial binding energy and the intrusion energy were analyzed to demonstrate that the dipping was a lift-off process and that the patterning complete was governed by the intrusion among pentacene, the substrate (hydrophilic or hydrophobic) and the D.I. water.

## 2. Experiments

In the patterning of the pentacene film, an attempt was made to control the surface polarity by exposure to UV light (wavelength: 175–285 nm, power: 40 mW, dose: 0.043 mW/

* Corresponding author. Tel.: +886 5131305; fax: +886 5737681.
  *E-mail address:* hsiaowen@mail.nctu.edu.tw (H.W. Zan).
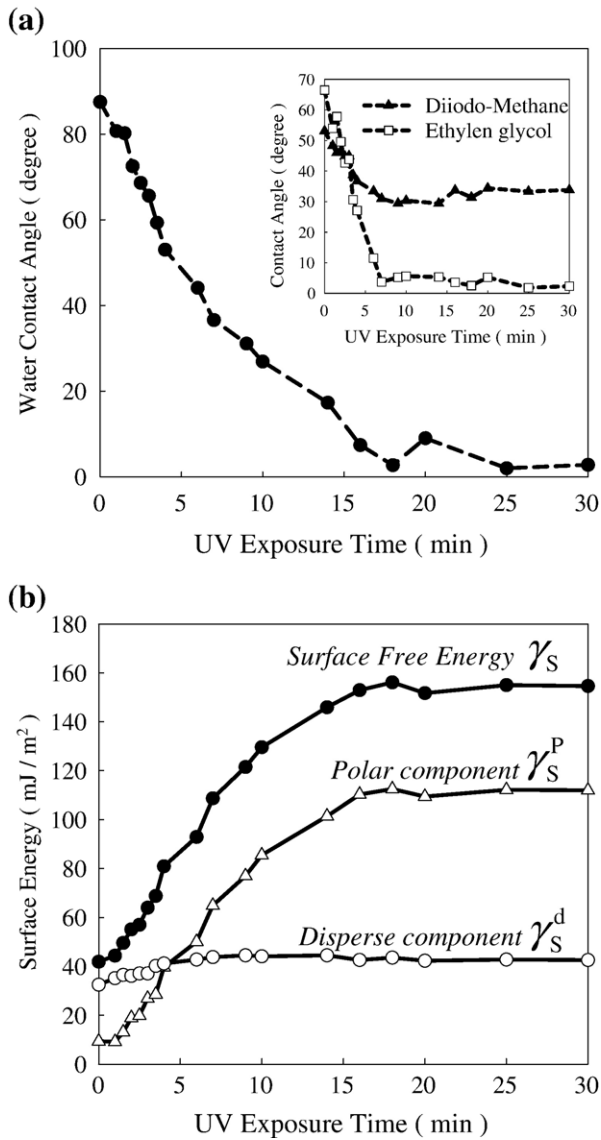
**(a)**



**(b)**



Fig. 1. Effect of exposure time to UV light on (a) the surface contact angle and (b) the polar and disperse components of the surface free energy following ODMS treatment.

cm$^2$). First, the silicon oxide was cleaned by acetone, isopropanol and acetone solution in that order. Then, the sample was dipped in the dissolved liquid ODMS to make the surface of the silicon oxide hydrophobic. The concentration of ODMS was 10 mM. Then, the surfaces were partially exposed to UV light for time varying from 0 to 30 min. As displayed in Fig. 1, the contact angle and the surface free energy were controlled by the duration of exposure to UV light. The contact angle was obtained by the Contact Angle System of KRÛSS for universal surface testing (model GH-100). Three standard liquids (D.I. water, diiodo-methane and ethylene glycol) were applied to measure contact angles and thus extract the surface free energy of the dielectric. Then, the surface free energy was calculated using the Fowkes and Young approximation [11,12].

To clearly compare the device characteristics, the device fabricating process was split into two parts. In the first part, the pentacene active region was defined by shadow mask. It was

deposited by thermal evaporation onto regions that had undergone ODMS treatment (Sample A) and onto regions that had undergone ODMS treatment followed by 30 min of exposure to UV (Sample B). The scale of shadow mask ranged from 300 μm to 700 μm and the scale of UV exposure mask was several centimeters. The thickness of the pentacene film was around 100 nm and the deposition rate was ~ 0.5 Å/s. 100 nm-thick Au pads were deposited through a shadow mask as source/drain contacts. Then, all of the samples were dipped in D.I. water and both the pentacene film and the source/drain contact in Sample B were lifted-off. Sample A′ refers to sample A after dipping in D.I. water to check the functionality of the transistors.

In the second part, the scale of the UV exposure mask ranged from 300 μm to 700 μm to define the pentacene active region without using the shadow mask. Sample A″ was the devices fabricated by the proposed lift-off method. The process conditions of Sample A″ were the same as those of Sample A′, except that the pentacene patterning methods was different. The width and length of the device channel were defined as 600 μm and 200 μm. An OTFT was fabricated using a conventional
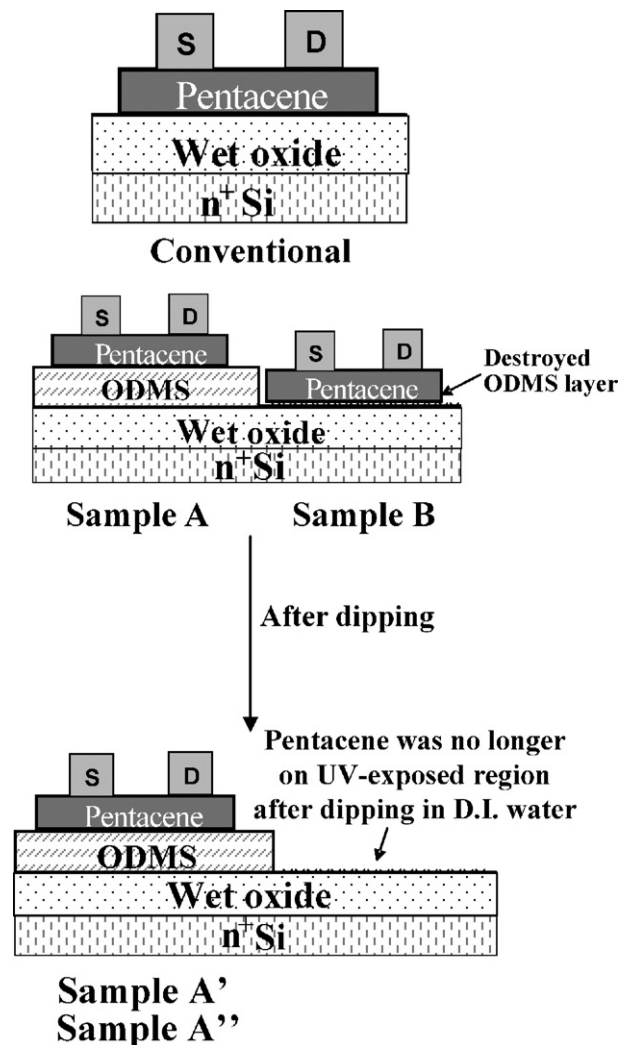


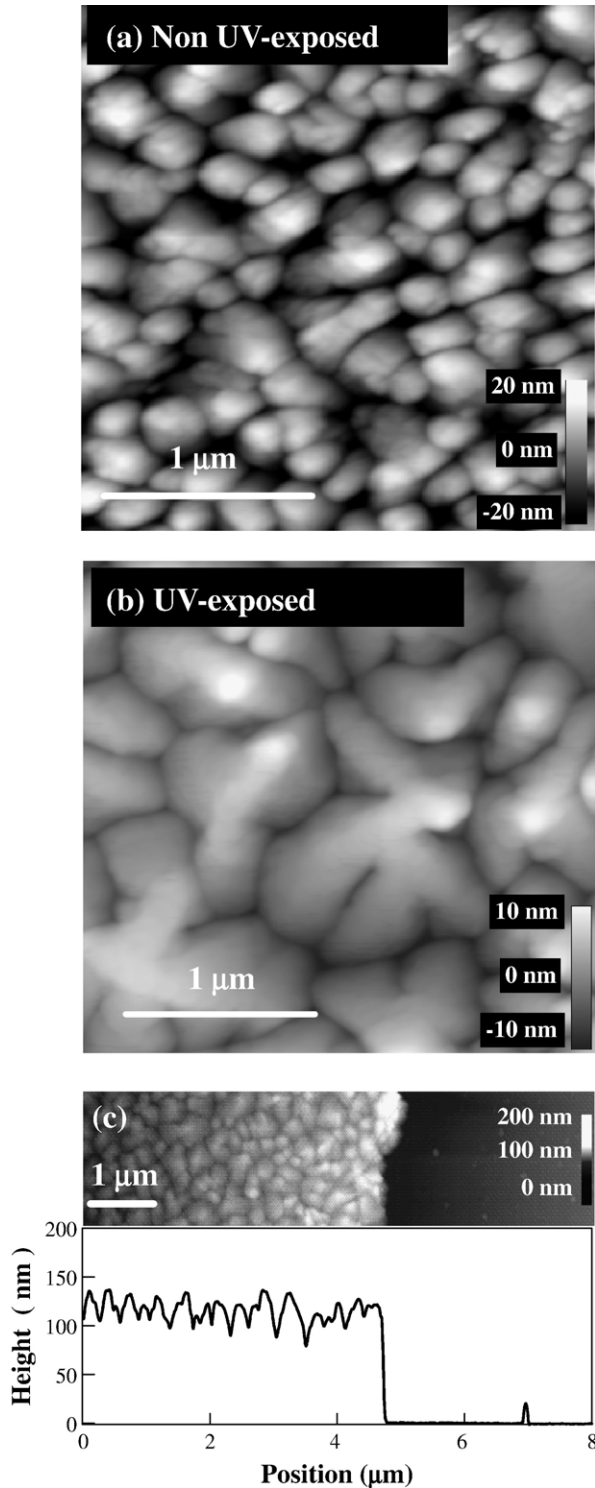Fig. 2. The fabricated OTFT under various conditions.

Fig. 3. AFM images of the pentacene deposited on (a) Non-UV-exposed and (b) 30-min UV-exposed regions of ODMS treated substrate and (c) image and height data of the intermediate region. The non-linear z-axis scale was shown in respective AFM images. In panel (c), the steps between these two areas were approximately 100 nm — similar to the thickness of the pentacene film, implying that the pentacene film was almost completely removed.

process without ODMS treatment or exposure to UV to serve as a control. This device was the conventional device. Fig. 2 schematically depicts devices with different conditions.

## 3. Results and discussion

### 3.1. Surface energy analysis

As presented in Fig. 1, the solid line represents the contact angle of the D.I. water with the dielectric surface. Before exposure to UV light, it was approximately 48.5° on bare $SiO_2$ and 90° on an ODMS-treated $SiO_2$ surface. Apparently, the ODMS transformed the $SiO_2$ surface from hydrophilic to hydrophobic. Following exposure to UV light, the contact angle decreased rapidly with time. After 600 s exposure, the contact angle dropped to be around 30°. After 25 min of exposure, the contact angle approached the limiting measurable angle of the instrument — about $5 \pm 5°$. Researchers have stated that UV light efficiently destroyed the organic film (ODMS) and altered the surface polarity [13]. The UV light excites such chemical bonds as C–C, C–H and C–Si, forming radicals [13]. Such radicals are active oxygen species such as ozone or atomic oxygen, which are generated by the excitation of atmospheric oxygen molecules by UV [13]:

$$O_2 + h\nu \rightarrow O(1D) + O(3P). \tag{1}$$
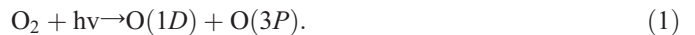
Hence, ODMS molecules may be converted to volatile species such as $CO_2$ and $H_2O$ that could be removed immediately [13].

The variation in the contact angle represented the change in surface energy. The surface energy was calculated using the Fowkes and Young approximation, as in the following equation [11,12];

$$(1 + \cos\theta)\gamma_L = 2(\gamma_S^d \gamma_L^d)^{1/2} + 2(\gamma_S^p \gamma_L^p)^{1/2} \tag{2}$$

where $\theta$ was the measured contact angle; $\gamma_L$ was the surface free energy of the testing liquid and was the sum of its dispersion part $\gamma_L^d$ and its polar part $\gamma_L^p$; $\gamma_S^d$ and $\gamma_S^p$ were the dispersion and polar components, respectively, of the surface free energy of the solid surface. The contact angles of three standard liquids (D.I. water, diiodo-Methane and ethylene
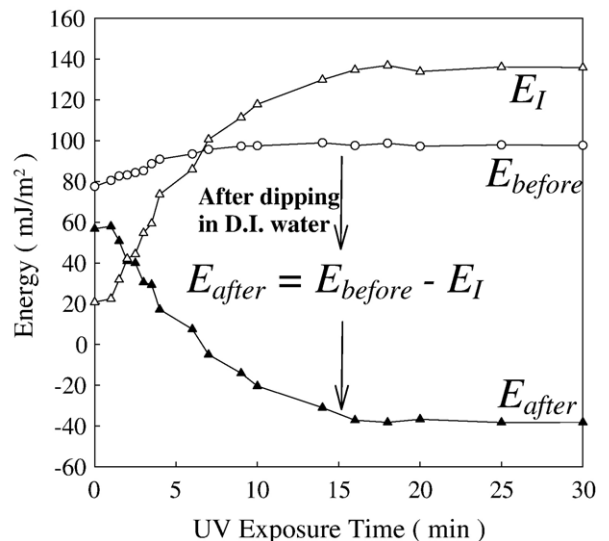


Fig. 4. Effect of exposure to UV light on the adhesion energy $E_{before}$, $E_{after}$ and intrusion energy $E_I$ following ODMS treatment.

glycol) were measured to obtain the values of $\gamma_S^d$ and $\gamma_S^p$. The inset of Fig. 1(a) plots the measurements. The $\gamma_L^d$ and $\gamma_L^p$ values of these standard liquids can be used to calculate the $\gamma_S^d$ and $\gamma_S^p$ values of the dielectric surface. Also, the total surface free energy of the solid $\gamma_S$ can be estimated by

$$\gamma_S \cong \gamma_S^p + \gamma_S^d. \qquad (3)$$

Fig. 1(b) plots the calculated results of $\gamma_S^d$, $\gamma_S^p$ and $\gamma_S$. UV light illumination changed mostly the polar component of the dielectric surface.

Table 1
Extracted parameters of OTFTs under various conditions

| | Conventional | Sample A | Sample B | Sample A′ |
|---|---|---|---|---|
| $\mu_{FE}$ (cm$^2$/V$_S$) | 0.17 | 0.26 | 0.11 | 0.22 |
| $V_{TH}$ (V) | − 6.7 | − 6 | − 7.34 | − 7.34 |
| $I_{on}/I_{off}$ | > 10$^5$ | ∼ 10$^8$ | ∼ 10$^5$ | > 10$^6$ |
| S.S. (V/dec.) | 1.73 | 0.69 | 3 | 0.74 |
| $N_{ss}$ (cm$^{-2}$ eV$^{-1}$) | 6.04 × 10$^{12}$ | 2.28 × 10$^{12}$ | 10.64 × 10$^{12}$ | 2.46 × 10$^{12}$ |

### 3.2. Adhesion energy analysis

Fig. 3(a) presents the atomic force microscopic (AFM) images of the pentacene deposited on the regions that had not been exposed to UV and that had been exposed to UV for 30 min. The AFM image was obtained by the tapping mode using an AFM model Dimension 3100, Digital Instrument. The AFM image demonstrated that the exposed pentacene had larger grains than the unexposed pentacene. This result agrees with results published [14] — that pentacene formed larger grains on surfaces of higher surface energy. Differences in surface energy led to different results after dipping in D.I. water. The AFM image in Fig. 3(b) reveals that, after dipping, the pentacene film on the non-exposed area was almost unchanged while that on the area that had been exposed to UV for 30 min was removed. The steps between these two areas were approximately 100 nm — similar to the thickness of the pentacene film, implying that the pentacene film was almost completely removed.

An attempt was made to characterize the adhesive properties of the pentacene film and the substrate surface to elucidate the patterning mechanism. The adhesion energy between materials, given by the following equations, has been presented elsewhere [15,16]:

$$E_{before} = 2\left(\sqrt{\gamma_{pe}^p \gamma_S^p} + \sqrt{\gamma_{pe}^d \gamma_S^d}\right) \qquad (4)$$

where $E_{before}$ denotes the adhesion energy between pentacene and the substrate before dipping in water; $\gamma_{pe}^p$ and $\gamma_{pe}^d$ are the polar component and the dispersion component of the surface energy of pentacene, and $\gamma_S^p$ and $\gamma_S^d$ are the polar component and the disperse component of the surface energy of the substrate. As displayed in Fig. 4, the adhesion energy before dipping in water was slightly increased after exposure to UV energy before dipping in water. This result was interesting since an increase in adhesion energy does not explain the water-removable characteristic.

Therefore, the intrusion energy $E_I$ caused by the interaction among water, pentacene and the dielectric surface was calculated. This intrusion energy causes a change in the adhesion energy:

$$E_{after} = E_{before} - E_I \qquad (5)$$

where $E_{after}$ denotes the adhesion energy after dipping in water. The intrusion energy is calculated using the following equation:

$$E_I = 2\left\{\sqrt{\gamma_{so}^p + \gamma_S^p} + \sqrt{\gamma_{so}^d \gamma_S^d} + \sqrt{\gamma_{pe}^p \gamma_{so}^p} + \sqrt{\gamma_{pe}^d \gamma_{so}^d} - \left[\gamma_{so}^p + \gamma_{so}^d\right]\right\} \qquad (6)$$
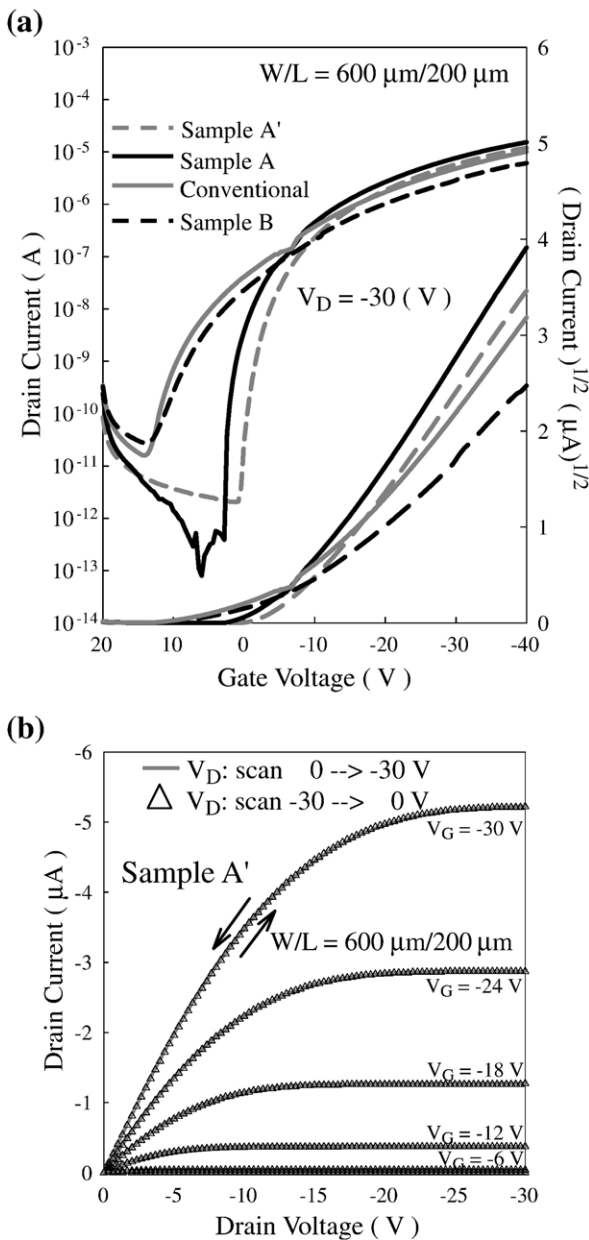


Fig. 5. (a) The transfer characteristics of various OTFT. Conventional devices were OTFT without any ODMS treatment or UV exposure. Sample A was with pentacene deposited onto ODMS-treated dielectric. Sample B was with pentacene deposited onto 30 min UV-exposed ODMS-treated dielectric. Sample A′ represents the sample A after the water dipping. (b) The output characteristics of sample A′.

where $\gamma_{so}^p$ and $\gamma_{so}^d$ are the polar and disperse components of the surface energy for the dipping solution, which was D.I. water herein. Fig. 4 also plots the calculated intrusion energy $E_I$ and the adhesion energy after dipping in water, $E_{after}$. $E_I$ increased significantly after exposure to UV light. Consequently $E_{after}$ fell to less than zero after exposure to UV. Specifically, the $E_{after}$ of the unexposed region was 58 mJ/m$^2$ and that of the region that had been exposed for 30 min was − 38 mJ/m$^2$. This fact explained the experimental results in Fig. 3(b). The unexposed area of the pentacene was almost unaffected because $E_{after}$ was large; the area of the pentacene film that had been exposed to UV for 30 min was removed by dipping in water because $E_{after}$ was negative. Also, the large difference between the $E_{after}$ of the unexposed area and that of the exposed area completely explained the capacity for patterning the pentacene film.
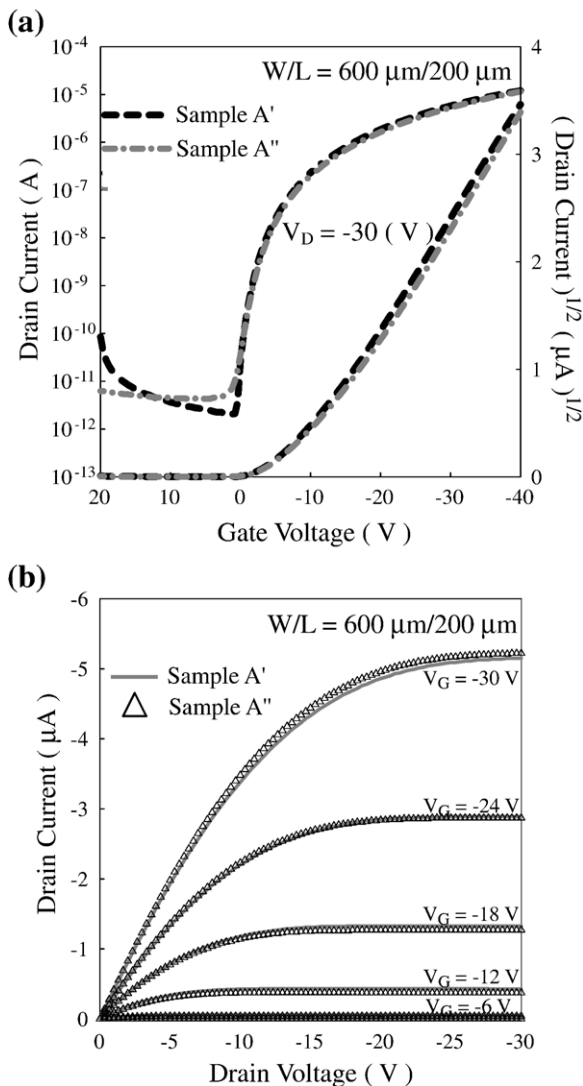


Fig. 6. (a) The transfer characteristics of various OTFT. Sample A′ was the device defined by shadow mask during pentacene evaporation. The pentacene in Sample A″ was patterned by the suggested method. (b) The output characteristics of sample A′ and Sample A″.

## 3.3. Device characteristic

The electronic characteristics were demonstrated to confirm that the patterning scheme was feasible for the OTFT. All electrical characteristics were measured using Agilent 4156 and Agilent 4284 analyzers. Fig. 5(a) compares the transfer characteristics of OTFT under different conditions. Table 1 lists the typical parameters such as mobility, threshold voltage, on/off current ratio, sub-threshold swing and the extracted interface state density ($N_{ss}$). The mobility and threshold voltage were extracted by the slope and the intercept of the square root of $I_D$ versus $V_G$ plot in Fig. 5. The interface state density was extracted by the method proposed in Ref. [17].

The ODMS-treated OTFT (Sample A) markedly outperformed the conventional devices without ODMS treatment. A steep subthreshold characteristic and a low interface trap density were obtained. High-quality, low-defect pentacene can be obtained if the surface energy of pentacene is matched to that of the dielectric [18]. The surface energy of the dielectric of Sample A was 41 mJ/m$^2$. This value matched the surface energy of pentacene and explained the good performance of Sample A.

Sample B with 30 min UV exposure after the ODMS treatment underperformed the conventional devices, indicating that 30 min of exposure to UV removed the ODMS layer. Additionally, extra defect states were created during long exposure to UV light. After dipping in water, Sample B was removed from the substrate and no electrical characteristics were obtained.

The characteristics of Sample A were analyzed after it was dipped in water, when the sample was denoted Sample A′. Sample A′ exhibited a similar mobility, subthreshold swing and interface state density as Sample A. Some residual water molecules may have been responsible for the slight increase in the threshold voltage and the off-state current, which phenomenon must be further studied. Fig. 5(b) plots the output characteristics of Sample A′. No hysteresis was observed when the drain voltage was scanned from 0 V to − 30 V and then from − 30 V to 0 V.

Finally, the transfer characteristic of Sample A″ were compared to those of Sample A′ in Fig. 6(a). The curves of the square root of $I_D$ versus $V_G$ were also plotted. Compare to Sample A′, an almost identical performance was obtained from Sample A″. For Sample A″, a mobility of 0.21 cm$^2$/Vs, a threshold voltage of around − 7.6 V and an on/off current ratio around six orders were obtained. The minimum drain current ($I_{min}$) of Sample A″ was a bit larger than that of Sample A′. Different remaining water content may be the plausible reason. As shown in Fig. 6(b), the output characteristics of Sample A″ was matched those of Sample A′. The results demonstrated the effectiveness of this pentacene patterning technology.

## 4. Conclusion

The surface energy of a gate dielectric was controlled for pentacene patterning using ODMS surface treatment, partial exposure to UV light and water dipping. The SiO$_2$ gate dielectric with ODMS treatment exhibited surface energy as low

as 41 mJ/m$^2$. The surface energy increased significantly when the ODMS-treated dielectric surface was irradiated by UV light (wavelength: 175–285 nm, power: 40 mW). After 30 min of exposure to UV, the surface energy increased to155 mJ/cm$^2$. The difference between the surface energies influenced the pentacene growth, the adhesion energy between pentacene and the dielectric surface and the intrusion energy when the pentacene was dipped in water. Even though the pentacene seemed to adhere most strongly to the dielectric surface after exposure to UV, it was easily removed by dipping in water because the high intrusion energy greatly reduced the adhesion energy. The pentacene on the non-UV-exposed area (low surface energy) remained unchanged during dipping in water. Pentacene-OTFT fabricated by the proposed method was characterized. After they had been dipped in water, a mobility of 0.21 cm$^2$/Vs, a threshold voltage of − 7.6 V and an on/off current ratio around six orders were obtained. The proposed technology is compatible with conventional lithography systems and is applicable to OTFT arrays.

## Acknowledgements

## References

[1] S.F. Nelson, Y.-Y. Lin, D.J. Gundlach, T.N. Jackson, Appl. Phys. Lett. 72 (1998) 1854.

[2] C. Goldmann, S. Haas, C. Krellner, K.P. Pernstich, D.J. Gundlach, B. Batlogg, J. Appl. Phys. 96 (2004) 2080.

[3] Hsiao-Wen Zan, Kuo-Hsi Yen, Pu-Kuan Liu, Kuo-Hsin Ku, Chien-Hsun Chen, Jennchang Hwang, Jpn. J. Appl. Phys. 45 (2006) 41.

[4] Iwao Yagi, Kazuhito Tsukagoshi, Yoshinobu Aoyagi, Appl. Phys. Lett. 86 (2005) 103502.

[5] Hsiao-Wen Zan, Kuo-Hsi Yen, Chien-Hsun Chen, Pu-Kuan Liu, Kuo-Hsin Ku, Jennchang Hwang, Electrochem. Solid-State Lett. 10 (2007) H8.

[6] M. McDowell, I.G. Hill, J.E. McDermott, S.L. Bernasek, J. Schwartz, Appl. Phys. Lett. 88 (2006) 073505.

[7] A. Inoue, T. Ishida, N. Choi, Appl. Phys. Lett. 73 (1998) 14.

[8] Sung Hwan Kim, Hye Young Choi, Seung Hoon Han, Ji Ho Hur, Jin Jang, Society for Information Display 2004, San Jose, CA, May 25–27, 2004. SID2004 Symposium Proceedings 45.2, 2004, p. 1297.

[9] Tetsu Tatsuma, Wakana Kubo, Akira Fujishima, Langmuir 18 (2002) 9632.

[10] Masahiko Ando, Masahiro Kawasaki, Shuji Imazeki, Hiroshi Sasaki, Toshihide Kamata, Appl. Phys. Lett. 85 (2004) 1849.

[11] Drew Myers, Surfaces, Interfaces, and Colloids: Principles and Applications, 2nd Edition, Wiley, New–York NY, 1999, p. 430.

[12] F.M. Fowkes, J. Phys. Chem. 67 (1963) 2538.

[13] H. Sugimura, N. Saito, N. Maeda, I. Ikeda, Y. Ishida, K. Hayashi, L. Hong, O. Takai, Nanotechnology 15 (2004) s69–s75.

[14] Sang Yoon Yang, Kwonwoo Shin, Chan Eon Park, Adv. Mater. 15 (2005) 1806.

[15] Hitoshi Nagata, Akira Kawai, Jpn. J. Appl. Phys. 28 (1989) 2137.

[16] D.H. Kaelble, J. Appl. Polym. Sci. 18 (1974) 1869.

[17] K.N. Narayanan Unni, Sylvie Dabos-Seignon, Jean-Michel Nunzi, J. Phys., D, Appl. Phys. 38 (2005) 1148.

[18] Wei-Yang Chou, Chia-Wei Kuo, Horng-Long Cheng, Yi-Ren Chen, Fu-Ching Tang, Feng-Yu Yang, Dun-Yin Shu, Chi-Chang Liao, Appl. Phys. Lett. 89 (2006) 112126.